Analytical Biochemistry 596 (2020) 113637

Contents lists available at ScienceDirect

Analytical Biochemistry

journal homepage: www.elsevier.com/locate/yabio

Lateral flow assay using aptamer-based sensing for on-site detection of dopamine in urine

Shima Dalirirad[a,b], Andrew J. Steckl[a,c,*]

[a] Nanoelectronics Laboratory, University of Cincinnati, Cincinnati, OH, 45255-0030, USA
[b] Department of Physics, University of Cincinnati, Cincinnati, OH, 45255-0030, USA
[c] Department of Electrical Engineering and Computer Science, University of Cincinnati, Cincinnati, OH, 45255-0030, USA

ARTICLE INFO

Keywords:
Dopamine
Urine
Aptamer
Au nanoparticle
Lateral flow assay
Duplex dissociation

ABSTRACT

A lateral flow assay using DNA aptamer-based sensing for the detection of dopamine in urine is reported. Dopamine duplex aptamers (hybridized sensor with capture probe) are conjugated to 40-nm Au nanoparticles (AuNPs) with 20T linkers. The detection method is based on the dissociation of the duplex aptamer in the presence of dopamine, with the sensor part undergoing conformational changes and being released from the capture part. Hybridization between the complementary DNA in the test line and the conjugated AuNP-capture DNA produces a red band, whose intensity is related to the dopamine concentration. The minimum detectable concentration obtained by ImageJ analysis was < 10 ng/mL (65.2 nM), while the visual limit of detection is estimated to be ~50 ng/mL (normal range of dopamine in urine of 52–480 ng/mL or 0.3–3.13 μM). No cross reactivity to other stress biomarkers in urine was confirmed. These results indicate that this robust and user-friendly point-of-care biosensor has significant potential for providing a cost-effective alternative for dopamine detection in urine.

1. Introduction

Biomarkers present in the body that are related to conditions of stress are very important diagnostic tools [1–3]. Recently, rapid and low-cost detection of stress biomarkers in biological fluids has received increasing attention [4–6]. An important biomarker is dopamine, a member of catecholamine neurotransmitter group that plays a significant function in human mental and physical processes [7]. Dopamine controls many biological functions, such as regulating movements, cognition, motivation, mood [8,9] and even addictive behaviors [7]. Disturbances in dopamine levels may lead to neurodegenerative diseases, such as Alzheimer's, Parkinson's and Huntington's diseases [10,11]. Individuals suffering from these diseases have lower dopamine concentrations in their body compared to healthy individuals [12]. Therefore, monitoring dopamine levels is important for early diagnostics and treatment of these diseases. The development of methods for simple and low-cost point-of-care measurement of dopamine levels could assist patients with impaired release of this important chemical by providing in-home self-monitoring.

Conventional methods utilized for the detection of dopamine and other biomarkers are relatively laborious techniques using sophisticated equipment and procedures, such as electrochemical detection [13–15], chemiluminescence [16,17], high performance liquid chromatography (HPLC) [18,19], colorimetry [20,21] and fluorescence [22,23]. These methods, while providing high sensitivity are not suitable for rapid on-site screening device for dopamine detection.

Microfluidic paper-based lateral flow assay (LFA) devices provide a robust, cost effective and user-friendly POC system to detect and measure the target biomarker [24]. LFAs have been used in a wide range of qualitative and semi-quantitative monitoring of protein biomarkers, pathogens and food allergens [25–27]. The antibody-antigen binding reaction is one of the most commonly employed detection methods in LFAs, with the pregnancy test kit being a very widely utilized example [28,29]. Antibodies have played a critical role in the research and development of biomarker diagnostics, but do exhibit some limitations, such as high immunogenicity, short shelf life, high cost, time-consuming production with variations in batches and reduced selectivity for low molecular weight compounds [30,31].

Recently, aptamers have been developed as alternative probes in LFAs and other formats. Aptamers are single strand DNA or RNA oligonucleotides (ssDNA, ssRNA) synthesized *in vitro* by sequential evolution of ligands by exponential enrichment (SELEX) process from an existing library of DNA or RNA molecules [30]. Aptamer-based lateral flow assays/sensors have been reported for the detection of proteins

* Corresponding author. Nanoelectronics Laboratory, University of Cincinnati, Cincinnati, OH, 45255-0030, USA.
E-mail address: a.steckl@uc.edu (A.J. Steckl).

https://doi.org/10.1016/j.ab.2020.113637
Received 8 November 2019; Received in revised form 14 February 2020; Accepted 16 February 2020
Available online 19 February 2020
0003-2697/

[32–34], cancer cells [35], toxins [36] and nucleic acids [37]. Aptamers are typically used in conjunction with gold nanoparticles (AuNPs) for simple yet sensitive colorimetric detection in POC devices [38]. Aptamer-modified AuNPs have been applied for the detection of various analytes [39,40] in biological fluids. Recent advances in aptamer-based LFAs can be found in the article by Jauset-Rubio et al. [41].

Among reports on dopamine detection using aptamers, they have been either not tested in biological fluids [17,20,42] or have not utilized POC-compatible platforms, such as LFA [43–46]. The goal of this work is to develop methods that could overcome these limitations by incorporating conjugated AuNP-aptamer in LFA platform. The proposed aptasensor allows for a sensitive and easy technique to detect and quantify dopamine *in vitro*. An aptamer with specific affinity to dopamine [47] was utilized in a duplex format with a partially complementary DNA. Increasing dopamine concentration in urine leads to increasing dissociation of the duplex and concomitant hybridization (and signal intensity) of the sensor DNA on the test line of the LFA. To the best of our knowledge, this is the first report of aptamer-based LFA strip biosensor for dopamine detection in urine. Urine has been selected as the biofluid to be investigated since dopamine is known to be stable in this medium [48].

2. Biosensor design principles

The duplex dissociation mechanism offers a useful approach for small molecules detection [47,49]. In this approach, a capture aptamer strand (DNA_3) that is attached to the AuNP via a 20T linker (DNA_1) can hybridize with a region of a free aptamer (DNA_2) in solution in order to act as a sensor probe. The thermodynamic stability of the hybridized duplex aptamer is tuned to result in dissociation in the presence of the target.

As illustrated in Fig. 1a, in the absence of the target the two strands are hybridized, while in presence of the target, the sensor probe undergoes conformational changes leading to dissociation from the capture probe (Fig. 1b). The binding reaction and displacement of the strands occur in the solution phase. The assay response in the LFA format is shown schematically in Fig. 2a, with both test and control lines functionalized with streptavidin and biotinylated complementary oligomers. Test and control zones contain $cDNA_3$ and $cDNA_1$ that are complementary to the capture part of the duplex and to the linker, respectively. When the sample solution contains dopamine, target interactions dissociate the DNA_2 from the conjugated thiol-capture probe, leading to the hybridization of the capture probe to its complementary strand in the test line (Fig. 2b). In the absence of the target, the capture probe remains as a part of the duplex and thus results in no hybridization with the immobilized complementary oligomer at the test zone (Fig. 2c). At the control line, a red band is produced by the hybridization between thiolated 20T and biotinylated 20A to indicate that the assay works properly.

3. Experimental

3.1. Materials and solutions

Dopamine aptamer, TE buffer pH 8 and nuclease-free (NF) water were purchased from Integrated DNA Technologies (Coralville, Iowa). 40 nm Au nanoparticles were purchased from Nanocomposix (San Diego, CA). Dopamine protein (≥98%) and cortisol protein (≥98%) were purchased from Fitzgerald (Acton, MA). Artificial urine was obtained from Pickering Laboratories (Mountain View, CA).

The following items were purchased from Millipore Sigma (St. Louis, MO): serotonin (≥98.0%), neuropeptide Y (NPY; human, ≥95%), sodium phosphate tribasic (Na_3PO_4• $12H_2O$), sodium chloride, magnesium chloride, Tween 20, Triton X-100, bovine serum albumin (BSA), cysteamine, sucrose, HCl, sodium saline citrate 20× (SSC), tris-2-carboxyethyl phosphine hydrochloride (TCEP), 6-mercapto-1-hexanol (MCH) and phosphate buffered saline (PBS). Tris buffer (pH 8), nitrocellulose (NC) membrane (Millipore HF135), and cellulose fiber sample pad (CFSP001700), were purchased from MilliporeSigma (St. Louis, MO). Glass fiber pads (8950) were purchased from Ahlstrom (Helsinki, Finland). Streptavidin was obtained from IBA (Göttingen, Germany). DNA Sequences used in this study are shown in Table 1.

3.2. Preparation of AuNPs-aptamer conjugate

The AuNPs-aptamer conjugates was prepared based on the covalent bond between the thiolated DNA strands and AuNPs via a gold-sulfur reaction. Briefly, prior to conjugation 5 μL thiolated aptamer 100 μM is folded into the tertiary structure by adding to 45 μL folding buffer (1 mM $MgCl_2$, 1X PBS pH 7.4). The solution is heated at 90 °C for 5 min and then allowed to cool down to room temperature for ~15 min. Fifty microliters of thiol aptamer (10 μM) is activated with 2 μL TCEP 20 mM and then incubated for 1 h at room temperature. The mixture of 40 μL AuNP (OD = 7.5) with 2 μL activated aptamer was incubated in dark ambient overnight (at least 8 h). The mixture is aged by adding NaCl 1 M in a dropwise fashion (0.5 μL) with a gentle vortex within a 20 min time interval until a final concentration of 200 mM NaCl was reached (see Supplementary Material Figs. S1 and S2). Adding salt in the aging process increases the concentration of counterions and reduces the repulsive force between the DNA strands, leading to higher DNA loading on the AuNP surface [50]. The freshly prepared mixture was refrigerated for 24 h. Unconjugated thiol-aptamers were removed by centrifugation at 12,000 rpm for 10 min. The pellets were washed with NF water for 3 cycles. To block unoccupied sites on the AuNPs surface, 2 μL MCH 28 μM was added to 50 μL conjugated AuNP-aptamer. After 1h incubation, the mixture was washed for 3 cycles at 12,000 rpm for 10 min to remove the excess MCH.

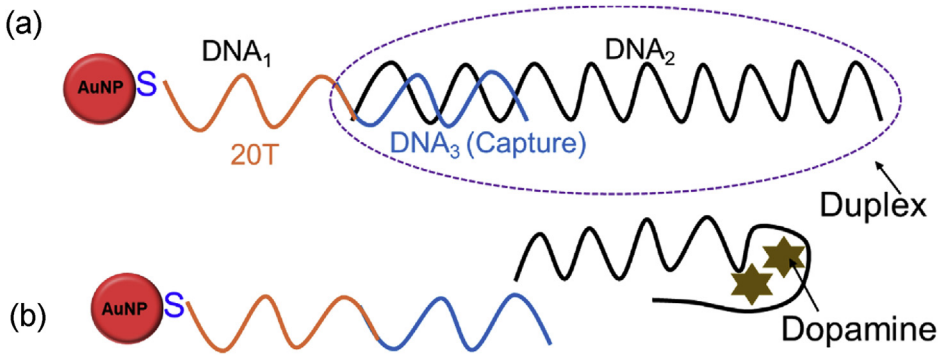

Fig. 1. DNA duplex dissociation approach: (a) AuNP functionalized with duplex strand; (b) aptamer dissociation from capture strand in presence of dopamine.

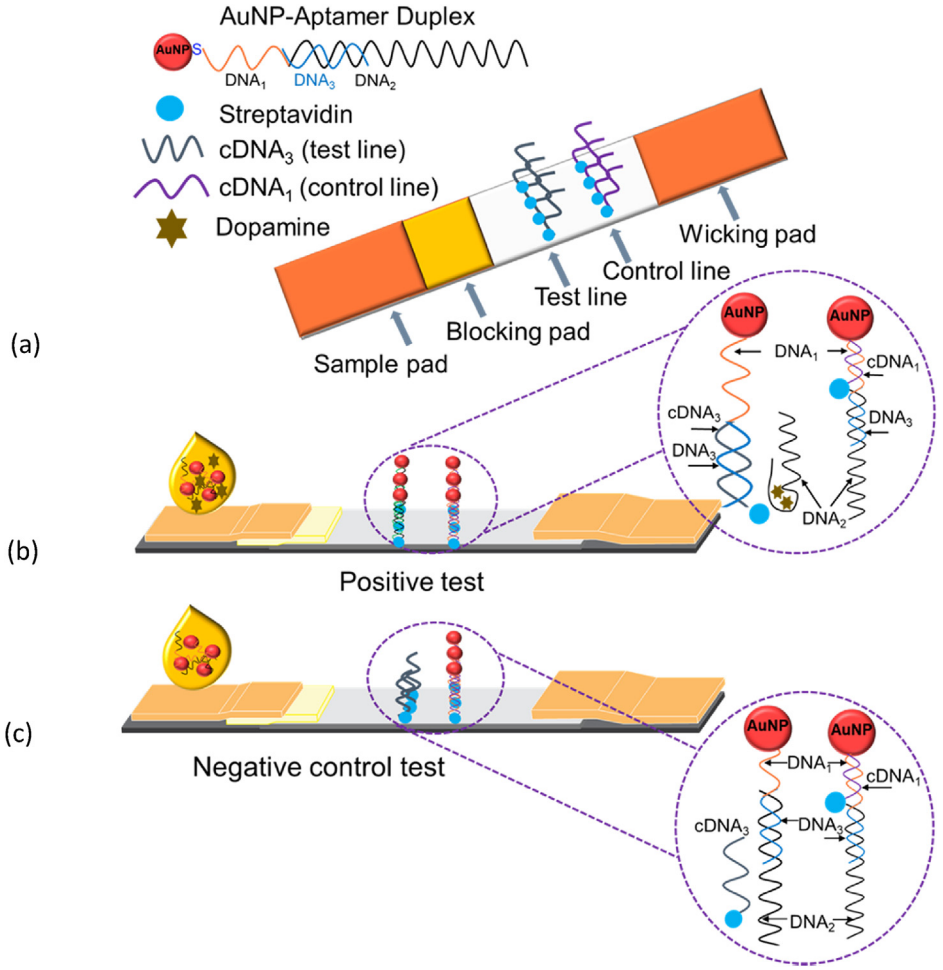

Fig. 2. Duplex dissociation design for aptamer-based lateral flow test strip: (a) structure of the test strips; (b) positive test in presence of dopamine; (c) illustration of the negative control.

Table 1
Sequences utilized in this study.

Name	Sequence (5' - 3')	# of bases
DNA_1	Thiol – TTT TTT TTT TTT TTT TTT TT	20
DNA_2	CTC TCG GGA CGA CGC GAG TTT GAA GGT TCG TTC GCA GGT GTG GAG TGA CGT CGT CCC	57
DNA_3	CGT CGT CCC GAG AG	14
$cDNA_1$	Biotin / AAA AAA AAA AAA AAA AAA AA	20
$cDNA_3$	Biotin / CTC TCG GGA CGA CG	14

3.3. Preparation of streptavidin-biotin-DNA conjugates

The *test line* solution was prepared by adding 69 μL biotin-complementary DNA (10 μM) into 23 μL streptavidin (1 mg/mL). Streptavidin was dissolved in PBS (pH 7.4) solution. The mixture was incubated at room temperature for 1 h and then centrifuged at 6000 rpm with a centrifugal filter (cutoff of 30 kDa, Millipore) for 20 min to remove excess aptamers. PBS was then added to the mixture up to its initial volume prior to centrifugation. The *control line* solution was prepared by adding an equal volume of streptavidin (1 mg/mL) to the control probe DNA (10 μM), followed by adding 12.5% SSC 20X into the solution after 1 h incubation in ambient. Optimization for the ratios of streptavidin to complementary DNA (cDNA) process were performed and the corresponding data is provided in the supplementary material (Figs. S3–S5).

3.4. Assembly of aptamer-based LFA strips and sample preparation

The test strip for dopamine detection in artificial urine consists of four components: sample pad, blocking agent pad, NC membrane (Millipore HF135 – 35 mm × 20 cm) and wicking pad. All four parts are mounted on an adhesive backing card with 2-mm overlap to ensure liquid transfer between the membrane and the pads. Individual test strips with dimensions of 5 mm × 60 mm were formed using a guillotine cutter (CM4000, BioDot, Irvine, CA). Complementary probes were dispensed (Biojet AD1500) in the test and control zones at 15 and 20 mm distance from the beginning of the NC membrane. The test line was formed by dispensing solution three consecutive times, with a drying step between each printing. The control line solution was dispensed in a single printing.

Sample pads (5 mm ×10 mm) were made from cellulose fiber membranes (CFSP001700) soaked in a buffer solution (0.15 mM NaCl, 0.05 M Tris and 0.25% Triton X-100 (pH 8). Blocking pads were soaked in a different buffer (5% BSA, 20 mM Na_3PO_4, 10% sucrose and finally adding 0.25% Tween20). Both pads were soaked for 30 min in their respective buffers and then dried at 45 °C for 90 min. The incorporated sample buffer in the sample pad assists the migration of the dispensed solution into the membrane. Blocking agents were used to reduce nonspecific binding of the aptamer to the NC membrane. To avoid the effect of moisture on flow rate, the test strips were dried at 60 °C for 10 min and stored at room temperature in boxes containing silica desiccant.

The aptamer-based test strip was applied to the analysis of

dopamine in urine samples. A dopamine protein stock solution was first prepared by dissolving 1 mg into 10 μL HCl 0.1 M and then 990 μL artificial urine is added. The solution is subsequently diluted with artificial urine for desired concentrations. 300 μL dopamine solutions in different concentrations were added to the (~5 μL) washed and blocked conjugated AuNP-aptamer pellets. Samples containing dopamine in different concentrations were incubated for 10 min at room temperature in dark ambient. 80 μL of solution were dispensed on the sample pad of the test strips and the results were recorded after 15 min.

4. Results and discussion

We have incorporated into our biosensor a dopamine aptamer reported by Nakatsuka et al. [47] to have a dissociation constant K_d of 150 nM. The overall sample preparation for the conjugation of AuNP-aptamers was the same as described above. Solutions of 80 μL with various dopamine concentrations were dispensed on sample pads of the test strips. The capture component of the synthesized dopamine aptamer followed the aptamer reported by Nakatsuka et al. [47]. We have incorporated the capture part as a complementary DNA on the test zone of the strip.

The principles and configuration for LFA-based detection using the dissociation of a duplex aptamer upon capture of dopamine was illustrated in Fig. 2. The direct local dispensing of DNA on NC membrane is not useful because the DNA molecules are washed away by the liquid sample migrating through the membrane. Streptavidin is known to be immobilized on NC membranes through electrostatic absorption. Biotinylated DNA_3 (complementary to capture DNA_2) was bound to streptavidin and immobilized on the test line. A separate control line, using streptavidin-biotin-20A as a complementary sequence to the 20T linker of DNA_1, is formed at a 5-mm distance from the test line.

Dispensing 80 μL of the final solution containing conjugated AuNP-duplex aptamer and dopamine in various concentrations produced a red band in the test zone through the hybridization between the conjugated aptamer to its immobilized complementary on the test zone. The excess conjugated AuNP-duplex molecules continue to flow through the membrane by capillary action. At the control zone hybridization between the control $cDNA_1$ probes (20A) and the linker on the AuNP duplex (20T) confirms the validity of the assay. As shown in Fig. 3a, at a dopamine concentration of 30 ng/mL the test line is very faint by visual observation, essentially the same as the control (no dopamine) case. The first clear visual observation of a red band at the test zone is at a concentration of 50 ng/mL. The test line color intensity is observed to increase with subsequent increasing dopamine concentrations in the sample tested up to 500–600 ng/mL. More accurate estimates of signal intensity were obtained using the ImageJ [51] program to measure the color intensity of each test line. The results are used to measure the intensities of the test lines by subtracting the background color. The resultant graph on Fig. 3b shows the mean value and standard error for each concentration calculated from 5 replicated experiments. The LOD based on ImageJ analysis is a few ng/mL (< 10 ng/mL). A fairly linear increase in signal is observed up to 500 ng/mL, beyond which saturation is observed.

Table 2
Stress biomarkers concentration ranges in urine under healthy physiological conditions [1].

Biomarker	Concentration in urine (ng/mL)
Cortisol	1–100
Dopamine	52–480
Epinephrine	0–20
Norepinephrine	15–80
Serotonin	5–23

To evaluate the specificity of the biosensor to dopamine, the test strips were challenged by other stress biomarkers that exist in urine: cortisol, epinephrine norepinephrine and serotonin. The ranges of healthy physiological concentrations of these biomarkers in urine are shown in Table 2 [4]. The same concentration of 500 ng/mL was used for all dispensed biomarkers. This is the high end of dopamine, and much higher than other normal concentration of stress biomarkers in human urine samples in order to have as challenging test as possible.

Assay preparation and measurement conditions were the same for all tests. A main urine solution (300 μL) was prepared for each biomarker at the same concentration of 0.5 μg/mL. Then ~5 μL of conjugated AuNP-duplex aptamer solution was added. After 10 min incubation in dark ambient, 80 μL of sample solution was dispensed on the test strip sample pad. 15 min after sample dispensing the results were recorded and analyzed. As shown in the inset photos of Fig. 4, a strong test line was observed for the dopamine test. For the other biomarkers, essentially no signal was visually observed. The intensity of the test line (peak area) was analyzed by ImageJ for 5 sets of experiments for each biomarker. The bar chart of Fig. 4 contains average detected peak areas of the test line for each biomarker along with the standard error. The signal from dopamine is seen to be ~10× that of the other biomarkers, which produced signals approximately the same as the control case. This result showed that the lateral flow test strips designed for dopamine detection in urine by incorporating the duplex aptamer can be used successfully for selective dopamine recognition.

4.1. Stability of test trips and conjugated AuNP-Aptamer solutions

The stability of the biosensor was considered. The stability of the conjugated AuNP-aptamer solutions was evaluated using optical

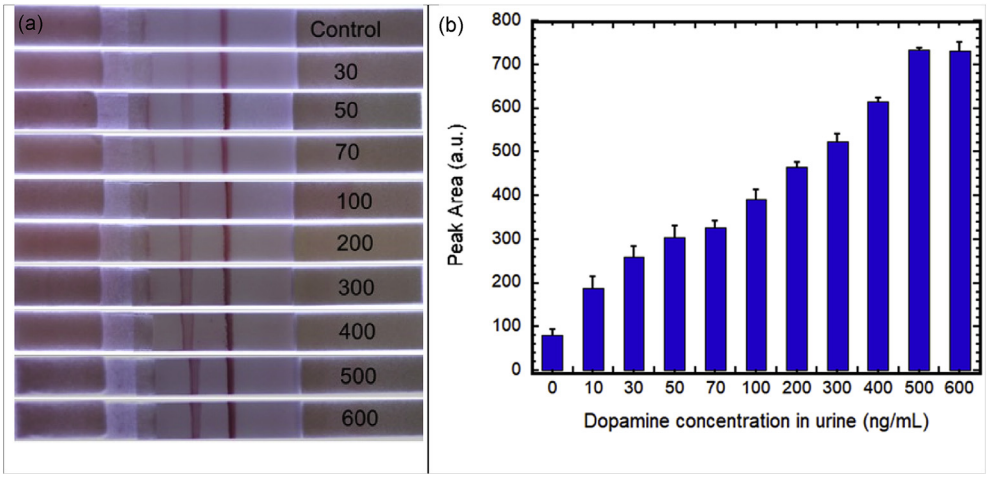

Fig. 3. Detection results of the test strips using duplex DNA aptamer sensing with different dopamine concentrations (ng/mL) in 80 μL test samples: (a) visual observation of the effect of dopamine concentration (control, 30–600 ng/mL) on color intensity of the test line; (b) peak area value of intensity calculated by ImageJ analysis to quantify dopamine presence (control, 10–600 ng/mL) at 15 min. Error bars indicate the standard error over five independent experiments. (For interpretation of the references to color in this figure legend, the reader is referred to the Web version of this article.)

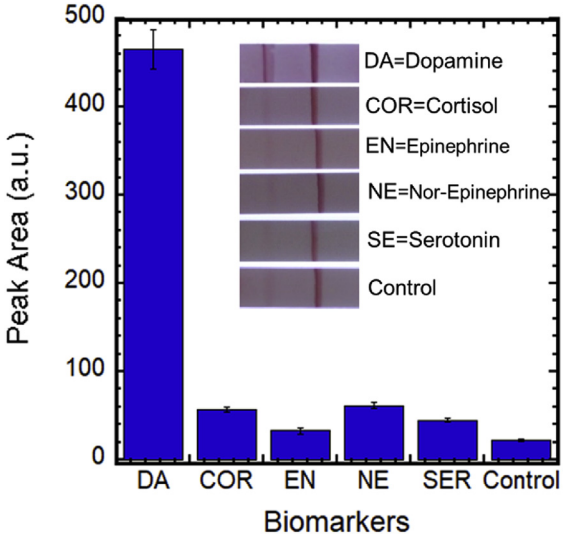

Fig. 4. Selectivity of the dopamine test strips in the presence of other stress biomarkers in urine (0.5 μg/mL, 80 μL) using ImageJ peak area detection: average and standard error for n = 5 replicates.

measurements (35 days) and the test strips were analyzed by ImageJ (30 days). To assess aptamer solution stability, 5 samples of conjugated AuNP-aptamer were prepared under the same procedure as described in Sec 3.2 by adding 2 μL duplex aptamer to 40 μL AuNP (OD = 7.5) followed by aging and blocking process. The samples were stored at 4 °C and the optical measurements were performed at 5-day intervals. As shown in Fig. 5a, all samples provided the same absorption at 260 nm (aptamer absorption) and 525 nm (AuNP absorption), indicating the stability of aptamers and AuNPs with no degradation or aggregation up to day 35. To measure the stability of the test strips, 50 strips were prepared by immobilizing the complementary DNA on the test and control lines. The as-prepared test strips from the same batch were stored in boxes containing silica desiccant to eliminate humidity side effects.

The intensity of the test lines was evaluated using ImageJ at 15 min after dispensing 80 μL samples containing 0.1 μg/mL dopamine in the urine, see Fig. 5b. Fully dried test strips formed by Day 2 provided a slightly higher intensity in test lines compared to Day 0. The intensity of the test lines started to decrease slightly after 25 days of storage in the nitrogen-filled box. As the aptamers have a quite long shelf-life stability, by changing the storage condition to a sealed bag containing silica desiccant packs, the stability of the test strips will increase to sufficient levels for commercial purposes.

5. Summary and conclusion

A simple, robust and user-friendly lateral flow test strip was successfully developed for the detection of dopamine in urine. Duplex dissociation presented a reliable approach for developing a test strip for small molecule detection such as dopamine. Dissociation of the aptamer from the duplex occurs in the presence of the target when the aptamer undergoes conformational changes. Therefore, increasing target concentration in the sample leads to greater dissociation and eventually increased binding in the test zone. ImageJ analysis of the limit of detection of dopamine in artificial urine on the test strip was found to be < 10 ng/mL while the visual LOD was ~50 ng/mL. The intensity of the test line increases nearly linearly with dopamine concentration in urine up to values of 500–600 ng/mL. This covers the reported physiological concentration range of dopamine in urine. The selectivity of the dopamine assay against other stress biomarkers was demonstrated. The test strip assay developed for dopamine detection in this study has strong potential for use as a reliable point-of-care device, with simple operation that can be completed in ~15 min.

CRediT authorship contribution statement

Shima Dalirirad: Methodology, Investigation, Writing - original draft, Writing - review & editing. **Andrew J. Steckl:** Conceptualization, Writing - review & editing.

Acknowledgments

The authors gratefully acknowledge many very helpful discussions with Daewoo Han, Michael C. Brothers, Mirelis Santos Cancel and Ryan White.

Appendix A. Supplementary data

Supplementary data to this article can be found online at https://doi.org/10.1016/j.ab.2020.113637.

Author contributions

The manuscript was written through contributions of both authors. Both authors have given approval to the final version of the manuscript.

Funding sources

This work was supported by the National Science Foundation and by the industrial members of the Center for Advanced Design and

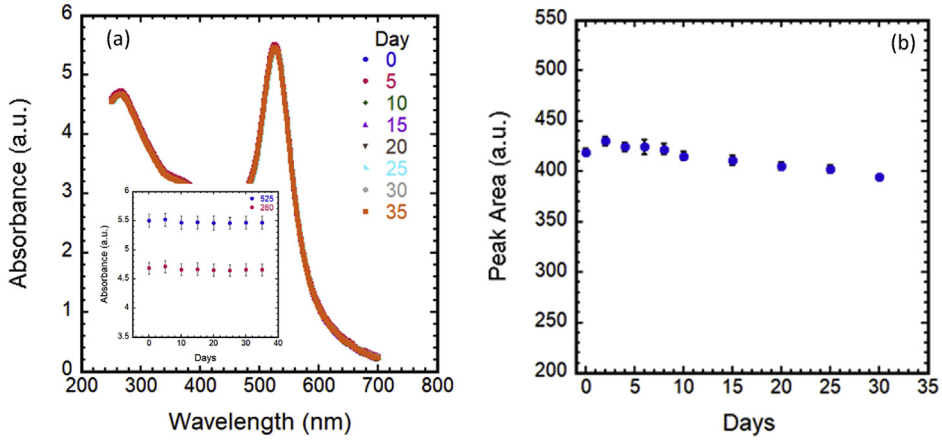

Fig. 5. Biosensor stability: (a) average optical absorption of 5 solutions at 260 and 525 nm over a period of 35 days; the figure insert shows the absorbance of aptamers at 260 nm and AuNPs at 525 nm as a function of time; (b) peak area intensity of test lines on test strips. Error bars indicate the standard error for n = 5.

Manufacturing of Integrated Microfluidics (NSF I/UCRC IIP-1738617) and by UES Inc. (S-104-000-001) as a subcontract from AFRL (FA8650-15-C-6631).

References

[1] A.P. Allen, P.J. Kennedy, J.F. Cryan, T.G. Dinan, G. Clarke, Biological and psychological markers of stress in humans: focus on the Trier Social Stress Test, Neurosci. Biobehav. Rev. 38 (2014) 94–124, https://doi.org/10.1016/j.neubiorev.2013.11.005.

[2] M.M. Bembea, N. Rizkalla, J. Freedy, N. Barasch, D. Vaidya, P.J. Pronovost, et al., Plasma biomarkers of brain injury as diagnostic tools and outcome predictors after extracorporeal membrane oxygenation, Crit. Care Med. 43 (2015) 2202–2211 https://doi:10.1097/CCM.0000000000001145.

[3] K.K. Wang, Z. Yang, T. Zhu, Y. Shi, R. Rubenstein, J.A. Tyndall, et al., An update on diagnostic and prognostic biomarkers for traumatic brain injury, Expert Rev. Mol. Diagn. 18 (2018) 165–180, https://doi.org/10.1080/14737159.2018.1428089.

[4] A.J. Steckl, P. Ray, Stress biomarkers in biological fluids and their point-of-use detection, ACS Sens. 3 (2018) 2025–2044, https://doi.org/10.1021/acssensors.8b00726.

[5] A. Kaushik, A. Yndart, R.D. Jayant, V. Sagar, V. Atluri, S. Bhansali, et al., Electrochemical sensing method for point-of-care cortisol detection in human immunodeficiency virus-infected patients, Int. J. Nanomed. 10 (2015) 677, https://doi.org/10.2147/ijn.s75514.

[6] A. Apilux, S. Rengpipat, W. Suwanjang, O. Chailapakul, Paper-based immunosensor with competitive assay for cortisol detection, J. Pharmaceut. Biomed. Anal. 178 (2020) 112925, https://doi.org/10.1016/j.jpba.2019.112925.

[7] M. Perry, Q. Li, R.T. Kennedy, Review of recent advances in analytical techniques for the determination of neurotransmitters, Anal. Chim. Acta 653 (2009) 1–22, https://doi.org/10.1016/j.aca.2009.08.038.

[8] J.A. Gingrich, M.G. Caron, Recent advances in the molecular biology of dopamine receptors, Annu. Rev. Neurosci. 16 (1993) 299–321, https://doi.org/10.1146/annurev.ne.16.030193.001503.

[9] V. Bassareo, G. Di Chiara, Differential responsiveness of dopamine transmission to food-stimuli in nucleus accumbens shell/core compartments, Neuroscience 89 (1999) 637–641, https://doi.org/10.1016/S0306-4522(98)00583-1.

[10] E.J. Nestler, Hard target: understanding dopaminergic neurotransmission, Cell 79 (1994) 923–926, https://doi.org/10.1016/0092-8674(94)90022-1.

[11] E. Farjami, R. Campos, J.S. Nielsen, K.V. Gothelf, J. Kjems, E.E. Ferapontova, RNA aptamer-based electrochemical biosensor for selective and label-free analysis of dopamine, Anal. Chem. 85 (2012) 121–128, https://doi.org/10.1021/ac302134s.

[12] B.-R. Li, Y.-J. Hsieh, Y.-X. Chen, Y.-T. Chung, C.-Y. Pan, Y.-T. Chen, An ultrasensitive nanowire-transistor biosensor for detecting dopamine release from living PC12 cells under hypoxic stimulation, J. Am. Chem. Soc. 135 (2013) 16034–16037, https://doi.org/10.1021/ja408485m.

[13] Y.-R. Kim, S. Bong, Y.-J. Kang, Y. Yang, R.K. Mahajan, J.S. Kim, et al., Electrochemical detection of dopamine in the presence of ascorbic acid using graphene modified electrodes, Biosens. Bioelectron. 25 (2010) 2366–2369, https://doi.org/10.1016/j.bios.2010.02.031.

[14] R. Li, T. Yang, Z. Li, Z. Gu, G. Wang, J. Liu, Synthesis of palladium@gold nanoalloys/nitrogen and sulphur-functionalized multiple graphene aerogel for electrochemical detection of dopamine, Anal. Chim. Acta 954 (2017) 43–51, https://doi.org/10.1016/j.aca.2016.12.031.

[15] B. Wei, H. Zhong, L. Wang, Y. Liu, Y. Xu, J. Zhang, et al., Facile preparation of a collagen-graphene oxide composite: a sensitive and robust electrochemical aptasensor for determining dopamine in biological samples, Int. J. Biol. Macromol. 135 (2019) 400–406, https://doi.org/10.1016/j.ijbiomac.2019.05.176.

[16] W. Gao, L. Qi, Z. Liu, S. Majeed, S.A. Kitte, G. Xu, Efficient lucigenin/thiourea dioxide chemiluminescence system and its application for selective and sensitive dopamine detection, Sensor. Actuator. B Chem. 238 (2017) 468–472, https://doi.org/10.1016/j.snb.2016.07.093.

[17] Y. Sun, Y. Lin, C. Ding, W. Sun, Y. Dai, X. Zhu, et al., An ultrasensitive and ultraselective chemiluminescence aptasensor for dopamine detection based on aptamers modified magnetic mesoporous silica @ graphite oxide polymers, Sensor. Actuator. B Chem. 257 (2018) 312–323, https://doi.org/10.1016/j.snb.2017.10.171.

[18] N. Li, J. Guo, B. Liu, Y. Yu, H. Cui, L. Mao, et al., Determination of monoamine neurotransmitters and their metabolites in a mouse brain microdialysate by coupling high-performance liquid chromatography with gold nanoparticle-initiated chemiluminescence, Anal. Chim. Acta 645 (2009) 48–55, https://doi.org/10.1016/j.aca.2009.04.050.

[19] M. Oh, E. Huh, M.S. Oh, J.-S. Jeong, S.-P. Hong, Development of a diagnostic method for Parkinson's disease by reverse-phase high-performance liquid chromatography coupled with integrated pulsed amperometric detection, J. Pharmaceut. Biomed. Anal. 153 (2018) 110–116, https://doi.org/10.1016/j.jpba.2018.02.025.

[20] Y. Zheng, Y. Wang, X. Yang, Aptamer-based colorimetric biosensing of dopamine using unmodified gold nanoparticles, Sensor. Actuator. B Chem. 156 (2011) 95–99, https://doi.org/10.1016/j.snb.2011.03.077.

[21] B. Kong, A. Zhu, Y. Luo, Y. Tian, Y. Yu, G. Shi, Sensitive and selective colorimetric visualization of cerebral dopamine based on double molecular recognition, Angew. Chem. 123 (2011) 1877–1880, https://doi.org/10.1002/anie.201007071.

[22] M. Shou, C.R. Ferrario, K.N. Schultz, T.E. Robinson, R.T. Kennedy, Monitoring dopamine in vivo by microdialysis sampling and on-line CE-laser-induced fluorescence, Anal. Chem. 78 (2006) 6717–6725, https://doi.org/10.1021/ac0608218.

[23] X. Chen, S. Chen, Q. Ma, Fluorescence detection of dopamine based on nitrogen-doped graphene quantum dots and visible paper-based test strips, Anal. Methods 9 (2017) 2246–2251 https://10.1039/C7AY00028F.

[24] A.W. Martinez, S.T. Phillips, G.M. Whitesides, E. Carrilho, Diagnostics for the developing world: microfluidic paper-based analytical devices, Anal. Chem. 82 (2010) 3–10, https://doi.org/10.1021/ac9013989.

[25] G.A. Posthuma-Trumpie, J. Korf, A. van Amerongen, Lateral flow (immuno) assay: its strengths, weaknesses, opportunities and threats. A literature survey, Anal. Bioanal. Chem. 393 (2009) 569–582, https://doi.org/10.1007/s00216-008-2287-2.

[26] A.B. Aissa, J. Jara, R. Sebastián, A. Vallribera, S. Campoy, M. Pividori, Comparing nucleic acid lateral flow and electrochemical genosensing for the simultaneous detection of foodborne pathogens, Biosens. Bioelectron. 88 (2017) 265–272, https://doi.org/10.1016/j.bios.2016.08.046.

[27] B.H. Park, S.J. Oh, J.H. Jung, G. Choi, J.H. Seo, E.Y. Lee, et al., An integrated rotary microfluidic system with DNA extraction, loop-mediated isothermal amplification, and lateral flow strip based detection for point-of-care pathogen diagnostics, Biosens. Bioelectron. 91 (2017) 334–340, https://doi.org/10.1016/j.bios.2016.11.063.

[28] K.M. Koczula, A. Gallotta, Lateral flow assays, Essays Biochem. 60 (2016) 111–120, https://doi.org/10.1042/EBC20150012.

[29] A.K. Yetisen, M.S. Akram, C.R. Lowe, Paper-based microfluidic point-of-care diagnostic devices, Lab Chip 13 (2013) 2210–2251, https://doi.org/10.1039/C3LC50169H.

[30] K.-M. Song, S. Lee, C. Ban, Aptamers and their biological applications, Sensors 12 (2012) 612–631, https://doi.org/10.3390/s120100612.

[31] A. Chen, S. Yang, Replacing antibodies with aptamers in lateral flow immunoassay, Biosens. Bioelectron. 71 (2015) 230–242, https://doi.org/10.1016/j.bios.2015.04.041.

[32] N.H.A. Raston, V.-T. Nguyen, M.B. Gu, A new lateral flow strip assay (LFSA) using a pair of aptamers for the detection of Vaspin, Biosens. Bioelectron. 93 (2017) 21–25, https://doi.org/10.1016/j.bios.2016.11.061.

[33] H. Xu, X. Mao, Q. Zeng, S. Wang, A.-N. Kawde, G. Liu, Aptamer-functionalized gold nanoparticles as probes in a dry-reagent strip biosensor for protein analysis, Anal. Chem. 81 (2009) 669–675, https://doi.org/10.1021/ac8020592.

[34] S. Dalirirad, A.J. Steckl, Aptamer-based lateral flow assay for point of care cortisol detection in sweat, Sensor. Actuator. B Chem. 283 (2019) 79–86, https://doi.org/10.1016/j.snb.2018.11.161.

[35] G. Liu, X. Mao, J.A. Phillips, H. Xu, W. Tan, L. Zeng, Aptamer− nanoparticle strip biosensor for sensitive detection of cancer cells, Anal. Chem. 81 (2009) 10013–10018, https://doi.org/10.1021/ac901889s.

[36] W. Zhou, W. Kong, X. Dou, M. Zhao, Z. Ouyang, M. Yang, An aptamer based lateral flow strip for on-site rapid detection of ochratoxin A in Astragalus membranaceus, J. Chromatogr. B 1022 (2016) 102–108, https://doi.org/10.1016/j.jchromb.2016.04.016.

[37] C. Zhu, Y. Zhao, M. Yan, Y. Huang, J. Yan, W. Bai, et al., A sandwich dipstick assay for ATP detection based on split aptamer fragments, Anal. Bioanal. Chem. 408 (2016) 4151–4158, https://doi.org/10.1007/s00216-016-9506-z.

[38] M. Cordeiro, F. Ferreira Carlos, P. Pedrosa, A. Lopez, P.V. Baptista, Gold nanoparticles for diagnostics: advances towards points of care, Diagnostics 6 (2016) 43, https://doi.org/10.3390/diagnostics6040043.

[39] J. Liu, Y. Lu, Preparation of aptamer-linked gold nanoparticle purple aggregates for colorimetric sensing of analytes, Nat. Protoc. 1 (2006) 246, https://doi.org/10.1038/nprot.2006.38.

[40] H. Xu, X. Mao, Q. Zeng, S. Wang, A.-N. Kawde, G. Liu, Aptamer-functionalized gold nanoparticles as probes in a dry-reagent strip biosensor for protein analysis, Anal. Chem. 81 (2008) 669–675, https://doi.org/10.1021/ac8020592.

[41] M. Jauset-Rubio, M.S. El-Shahawi, A.S. Bashammakh, A.O. Alyoubi, Advances in aptamers-based lateral flow assays, Trac. Trends Anal. Chem. (2017), https://doi.org/10.1016/j.trac.2017.10.010.

[42] W. Hu, Y. Huang, C. Chen, Y. Liu, T. Guo, B.-O. Guan, Highly sensitive detection of dopamine using a graphene functionalized plasmonic fiber-optic sensor with aptamer conformational amplification, Sensor. Actuator. B Chem. 264 (2018) 440–447, https://doi.org/10.1016/j.snb.2018.03.005.

[43] J.-J. Feng, H. Guo, Y.-F. Li, Y.-H. Wang, W.-Y. Chen, A.-J. Wang, Single molecular functionalized gold nanoparticles for hydrogen-bonding recognition and colorimetric detection of dopamine with high sensitivity and selectivity, ACS Appl. Mater. Interfaces 5 (2013) 1226–1231, https://doi.org/10.1021/am400402c.

[44] Y. Cao, M.T. McDermott, Femtomolar and Selective Dopamine Detection by a Gold Nanoparticle Enhanced Surface Plasmon Resonance Aptasensor, bioRxiv, 2018, p. 273078, https://doi.org/10.1101/273078.

[45] I. Álvarez-Martos, R. Campos, E.E. Ferapontova, Surface state of the dopamine RNA aptamer affects specific recognition and binding of dopamine by the aptamer-modified electrodes, Analyst 140 (2015) 4089–4096, https://doi.org/10.1039/C5AN00480B.

[46] I. Álvarez-Martos, A. Møller, E.E. Ferapontova, Dopamine binding and analysis in undiluted human serum and blood by the RNA-aptamer electrode, ACS Chem. Neurosci. 10 (2019) 1706–1715, https://doi.org/10.1021/acschemneuro.8b00616.

[47] N. Nakatsuka, K.-A. Yang, J.M. Abendroth, K.M. Cheung, X. Xu, H. Yang, et al., Aptamer–field-effect transistors overcome Debye length limitations for small-molecule sensing, Science 362 (2018) 319–324, https://doi.org/10.1126/science.aao6750.

[48] M. Nichkova, P.M. Wynveen, D.T. Marc, H. Huisman, G.H. Kellermann, Validation of an ELISA for urinary dopamine: applications in monitoring treatment of dopamine-related disorders, J. Neurochem. 125 (2013) 724–735, https://doi.org/10.1111/jnc.12248.

[49] K.-A. Yang, H. Chun, Y. Zhang, S. Pecic, N. Nakatsuka, A.M. Andrews, et al., High-affinity nucleic-acid-based receptors for steroids, ACS Chem. Biol. 12 (2017) 3103–3112, https://doi.org/10.1021/acschembio.7b00634.

[50] S.J. Hurst, A.K.R. Lytton-Jean, C.A. Mirkin, Maximizing DNA loading on a range of gold nanoparticle sizes, Anal. Chem. 78 (2006) 8313–8318, https://doi.org/10.1021/ac0613582.

[51] C.A. Schneider, W.S. Rasband, K.W. Eliceiri, NIH Image to ImageJ: 25 years of image analysis, Nat. Methods 9 (2012) 671, https://doi.org/10.1038/nmeth.2089.

Lateral Flow Assay Using Aptamer-Based Sensor for On-Site Detection of Dopamine in Urine

Shima Dalirirad [a,b] *and Andrew J. Steckl* [a,c*]

[a]Nanoelectronics Laboratory, [b]Department of Physics, [c]Department of Electrical Engineering and Computer Science, University of Cincinnati, Cincinnati, OH, 45255-0030, USA

Supplementary Material

Optimizing the loading density of aptamer on AuNPs surface.

For the optimum concentration of aptamer in AuNP solution, aptamer (10 μM) in different volumes (10, 8, 6, 4 and 2μl) was added to the 40μL AuNPs (OD=7.5). The optimization was performed based on obtaining good visual intensity of a red band for the test line in control samples (no dopamine). After dispensing 80μL sample solutions (conjugated AuNP-aptamer) on the sample pad, the intensity of the control line decreased for the sample contained 2 μL of 10 μM aptamer. It was found out that the 2 μL aptamer is sufficient for providing hybridization in the test zone. The minimum amount of loading density was required for increasing the assay sensitivity. Overloading of aptamers on AuNPs surface requires more dopamine in sample, which leads to a lower sensitivity of the assay. By decreasing the aptamer volume to 1.5 or 1 μL in 40 μL AuNPs, the solutions aggregated in the aging process.

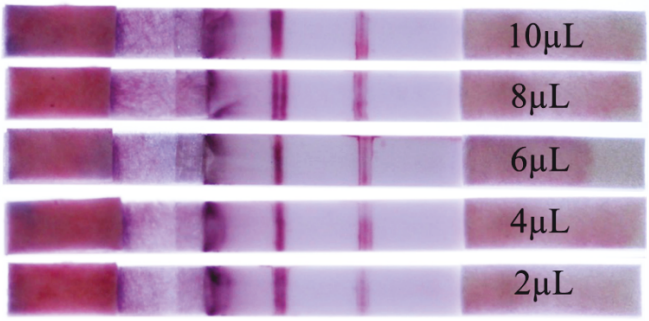

Fig. S1 Optimizing the loading density of aptamer on AuNPs solutions - adding different volumes (10, 8, 6, 4 and 2μL) of dopamine aptamer 10μM solutions into 40μL AuNPs solution.

After optimizing the final concentration of aptamers (476 nM) in conjugated AuNP-aptamer solution, NaCl at different concentrations (0, 40, 60, 80, 100, 120, 160, 200 and 220 mM) was added to the solutions. To find out the optimum concentration of NaCl needed for aging, 0.5 μL NaCl (1M) was added dropwise every 20 min to the solutions. After aging and incubation for at least 12 h at 4°C, the samples were centrifuged at 12000 rpm for 10 min. Then the supernatant was characterized by UV-Vis spectrometry for free aptamers absorption. As shown in Fig. S2, increasing the amount of salt in solutions results in a monotonic decrease in the absorbance at 260nm, which indicates the decrease of free aptamers in solutions and an increasing loading density of aptamers on AuNPs surface.

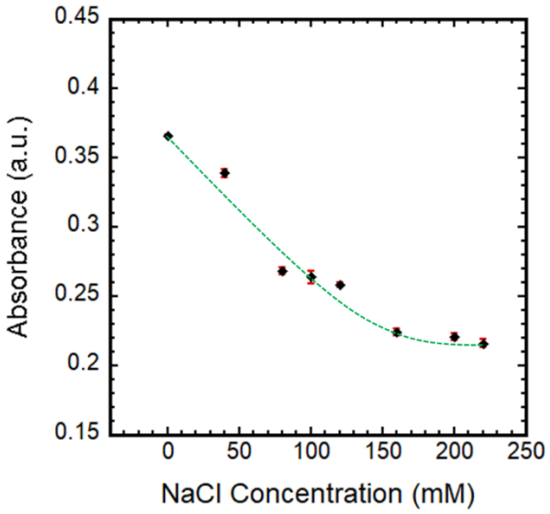

Fig. S2 UV-Vis spectra at λ = 260 nm for optimizing the NaCl in solutions for stabilizing the conjugated AuNP-aptamer at different concentrations (0, 40, 60, 80, 100, 120, 160, 200 and 220 mM).

The concentration of free aptamers in supernatant did not show much additional change by adding more than ~150-200 mM NaCl in samples. Therefore, 200mM was chosen as the optimum amount of NaCl in solution for aging process.

Preparation and Optimization of the test and control zone

To optimize the hybridization of conjugated aptamer to its complementary DNA string on the test and control lines, the ratio of streptavidin to complementary DNA was investigated. Streptavidin (1mg/mL, in PBS) was added to complementary DNA (C-DNA) 10μM in different volume ratios (2:1, 1:1, 1:2, 1:3, 1:4, 1:6) of streptavidin to C-DNA. Streptavidin and C-DNA were prepared in PBS and TE buffer, respectively, and then dispensed by Biojet for immobilizing on the nitrocellulose membrane. As shown in Fig. S3, the ratio of 1:3 streptavidin to C-DNA provides good performance of red band intensity in both test and control zones.

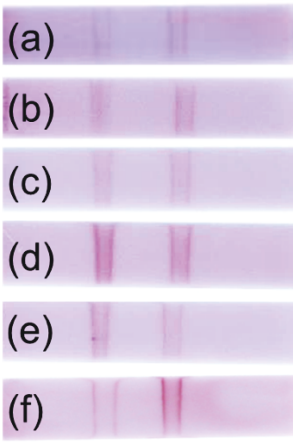

Fig. S3 Optimization the molar ratio of streptavidin to biotin complementary aptamer in test and control lines: (a) 2:1; (b)1:1; (c)1:2; (d)1:3; (e)1:4; (f) 1:6.

The intensities of the red bands in both test and control lines depend on the capture of the conjugated AuNPs. To obtain a sharp line with good intensity in both control and test zones, PBS, saline-sodium citrate (SSC) 20× and a combination of the two were investigated to provide no spreading effects, faster hybridization and having no negative effects on assay sensitivity. The initial steps of preparation the test and control line solutions were conducted as described in the main text. The buffers were added to the solutions after 1h incubation in ambient and centrifuging. As shown in Fig. S4a, both test and control lines which were produced using PBS experienced some spreading effect. Three consecutive dispensing steps with 10 min time interval between each printing for immobilizing were needed to provide good hybridization. Incorporating SSC 20× in both test and control line dispensing solutions eliminated the need for multiple line printing on test and control zones as it provided a sharp band with a good intensity in a single printing step. However, the use of SSC 20x led to a reduction in assay sensitivity. As shown in Fig. S4b,

resuspending the conjugated streptavidin-C DNA with SSC 20× results in hybridization and line formation in the test region even in the case of a sample containing high dopamine concentration (0.5 mg/mL). On the other hand, utilizing PBS for resuspension of centrifuged samples results in no line formation and thus could maintain the sensitivity of test strips (Fig. S4a).

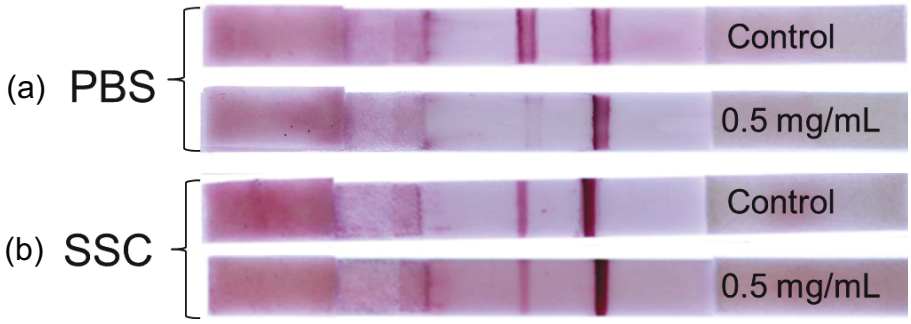

Fig. S4 Investigating buffers for providing a sharp band in test and control zones by testing sensitivity with 0 and 0.5 mg/mL dopamine in artificial urine; test and control zones made with (a) PBS, (b) SSC 20×.

Further studies were performed to determine the effect of reducing the concentration of SSC 20×. As shown in Fig. S5, decreasing the final concentration of SSC 20× in test line solutions even down to 1% still results in some level of C-DNA hybridization with conjugated aptamer-AuNP for control samples (which do not contain dopamine). Therefore, while the use of SSC 20× does improve the line formation, it has a negative effect on assay sensitivity even at greatly reduced concentrations in the final solution. Therefore, incorporation of SSC 20× use was limited to the control line, while the test line solutions were made using PBS.

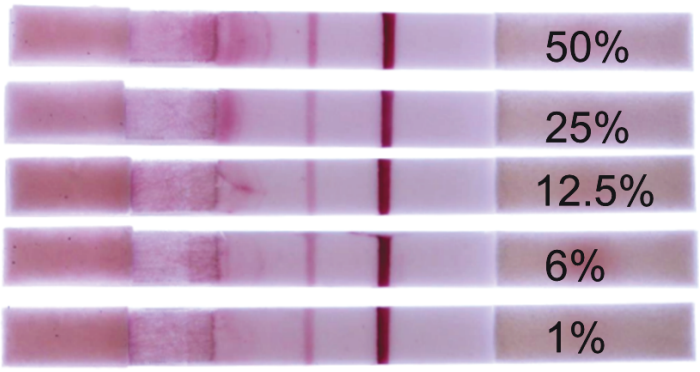

Fig. S5 Investigating the effect of reducing concentrations of SSC 20× in test line solutions.